

Visualization of the Material Flow in AA2195 Friction-Stir Welds Using a Marker Insert Technique

T.U. SEIDEL and A.P. REYNOLDS

The material flow in solid-state, friction-stir, butt-welded AA2195-T8 was investigated using a marker insert technique (MIT). Markers made of AA5454-H32 were embedded in the path of the rotating friction stir welding (FSW) tool and their final position after welding was detected by metallographic means. Changes in material flow due to welding parameter and tool geometry variations were examined. The method provides a semiquantitative, three-dimensional view of the material transport in the welded zone. Because of the placement of markers at different positions at the weld centerline, the material transport in the longitudinal, transverse, and the vertical directions could be studied. Markers embedded in the path of the tool remain continuous after welding. The material transport, which is not symmetrical about the weld centerline, was such that the bulk of the material was transported to a position behind its original position. Superimposed on the primary motion of material in the horizontal plane of the weld is a circulation about the longitudinal axis of the weld. This circulation is found to increase with increasing weld energy.

I. INTRODUCTION

FRICITION Stir Welding (FSW), developed at The Welding Institute (Cambridge, UK) in 1991,^[1] is especially well suited for joining high-strength aluminum alloys. The FSW process is a solid-state joining process combining friction, deformation heating, and mechanical work to obtain high-quality, defect-free joints. The required heat is produced during transport of material from the two plates to be joined around a nonconsumable, rotating tool. The shape of the tool promotes a high hydrostatic pressure along the joint line, causing consolidation of the material plasticized due to heat generation. Although significant effort has been expended in putting FSW to use in the full-scale production of such products as ferry boats, rocket fuel, and oxidizer tanks, the operating mechanisms and, in particular, the material flow during FSW are not fully characterized.

The microstructure of a typical FSW has been described in numerous previous publications^[2-6] but will be briefly reviewed here. Figure 1 shows the microstructure resulting from the FSW of AA2195-T8. The weld microstructure features can be separated into two broad categories: the thermomechanically affected zone (TMAZ), and the heat-affected zone (HAZ). This HAZ is similar to HAZs resulting from conventional, fusion welding processes. Depending on the alloy, its initial heat treatment, and the proximity to the weld centerline, processes occurring in the FSW HAZ might include precipitate coarsening, precipitate dissolution, recovery, recrystallization, and grain growth. The TMAZ of a friction stir weld might be considered analogous to the fusion zone of a conventional weld except that, instead of being melted, the material in the TMAZ has been mechanically worked.

Within the TMAZ, there are three somewhat distinct regions. The first and most obvious is the "weld nugget."

The weld nugget is the region that has undergone the most severe plastic deformation and is characterized by a fine, relatively equiaxed, recrystallized grain structure. The width of the nugget is normally similar to, but slightly greater than, the diameter of the pin. Outside of the nugget on either side is a second region, one that has been deformed to a lesser extent and that, depending on the alloy, may or may not show signs of recrystallization. In Figure 1, the delineation between the nugget and the rest of the TMAZ is quite sharp because of the recrystallization resistance of the AA2195-T8 base metal. The deformation of the base metal grains manifests itself as bending in the plane of the metallographic section (the grains are also bent in the horizontal plane perpendicular to the section). The third region of the TMAZ is the "flow arm." This is the region of material above the nugget. The flow arm is formed when the rotating tool shoulder passes over the weld. It should be noted that the FSW process is not symmetric about the centerline: the advancing side of the weld is defined as the side on which the rotational velocity vector of the welding tool has the same sense as the translational velocity vector of the tool relative to the workpiece. The retreating side is where the two vectors are of opposite senses. The leading side is the front of the tool and the trailing side indicates the back of the tool. The crown is the top surface of the weld and the root is the bottom surface.

II. BACKGROUND—FSW FLOW VISUALIZATION

Several friction stir weld flow visualization studies have been conducted. Midling^[6] investigated the influence of the welding speed on the material flow in welds of dissimilar aluminum alloys. He was the first to report on interface shapes using images of the microstructure. The flow visualization, however, was limited because no other detail except the interface between dissimilar alloys was investigated. Li *et al.*^[7] described patterns observed on metallographic cross sections in friction stir welds made both between dissimilar aluminum alloys and between aluminum alloys and copper.

T.U. SEIDEL, Graduate Research Assistant, and A.P. REYNOLDS, Associate Professor, are with the Department of Mechanical Engineering, University of South Carolina, Columbia, SC 29208.

Manuscript submitted February 1, 2001.

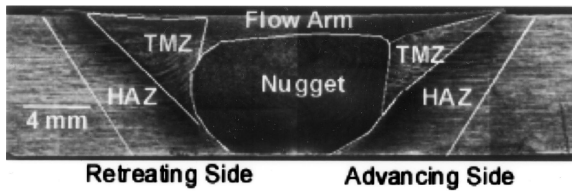


Fig. 1—Typical microstructure of an AA2195-T8 FSW.

The material flow was described as a chaotic-dynamic mixing. Colligan^[8] studied the material flow using embedded steel spheres placed along the weld centerline prior to welding. Colligan reported that material is stirred only in the upper portion of the weld and that in the rest of the weld, material is simply extruded around the pin. Colligan's approach of flow visualization, although elegant, was limited by following only single points in the weld. The chaotic mixing of stirred material that Colligan discovered may be a result of the finite size of the spheres. However, it must be stated that the details of the material flow are dependent on the exact tool geometry and welding parameters used; therefore, the generality of any conclusions about the material flow has not been established.

Reynolds *et al.*,^[9] Reynolds,^[10] and Seidel and Reynolds^[11] have analyzed the material flow of AA2195-T8 in several friction stir welds using a marker insert technique (MIT). This method is based on a postweld determination of the position of AA5454-H32 markers placed in the faying surface of the welded plates. The MIT allows the determination of the positions of material pre- and postwelding in the TMAZ through a serial sectioning technique. As a result, full three-dimensional plots of the deformed markers are obtained. They provide a good qualitative characterization of the material flow in friction stir welds. An extended analysis of the material flow in friction stir welded AA2195-T8 performed with different welding parameters and tool geometries is presented in this article.

III. PROCEDURE

A. Friction Stir Welding

The friction stir welds investigated in this research are butt-welded plates of 8.1-mm-thick AA2195-T8, an aluminum-lithium alloy with a nominal composition of 4.0Cu-1.0Li-0.5Mg-0.4Ag-0.12Zr-balance Al. The full-penetration, single-pass welds were performed on a vertical milling machine. The steps required to make a friction stir weld are as follows. First, the two pieces to be joined are clamped on a backing plate to hold the plates in place during welding. Second, the rotating tool, which consists of a broad shoulder and a narrower, threaded pin, is plunged into the faying surface of the two plates until the shoulder contacts the upper workpiece surface. The end of the plunging step corresponds to a constant initial backing-plate-to-pin clearance of 0.08 mm with the milling machine unloaded. Third, the rotating tool traverses along the centerline, which describes the original interface of the two plates, forming a joint. The tool-to-workpiece angle was 2.5 deg from the vertical axis in all welds. Figure 2 is a schematic showing the welding setup.

For each weld made, the pin diameter and weld pitch are listed in Table I. Common features for all tools include a

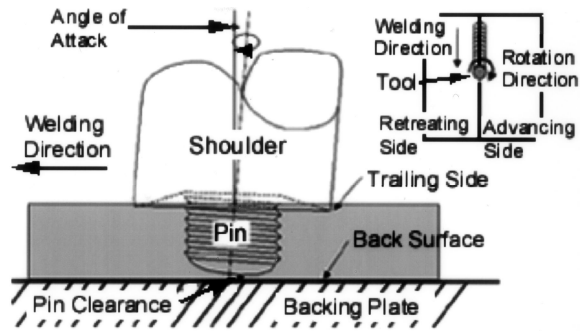


Fig. 2—Schematic drawing of the welding setup and process terminology.

Table I. Tool and Weld Parameter Details

Weld	Pin Diameter (mm)	Weld Pitch (mm/rev)	Description
1	9.9	0.61	cold
2	9.9	0.5	nominal (cold)
3	9.9	0.35	nominal (hot)
4	9.9	0.19	hot
5	7.8	0.61	cold
6	12.0	0.61	cold

shoulder diameter of 25.4 mm, pins threaded with a standard machine screw type thread and a thread pitch of 0.8 threads/mm, a shoulder dish angle of 7 deg (concavity), a pin length of 7.9 mm, and a pin tip radius of 8 mm. The weld pitch is defined as the tool advance per rotation (welding speed/rotational speed). It has been found that, in general, the specific weld energy (Joules/meter) correlates with the weld pitch,^[12] *i.e.*, the energy per unit length of weld increases as the weld pitch decreases. Therefore, welds with a low weld pitch are described as “hot” welds, while those with a relatively high weld pitch are described as “cold” welds. However, although the weld pitch is an important factor, welds made with the same pitch may have differing energy inputs; in particular, for two welds with the same weld pitch, the weld with the higher welding speed and rpm will in general be colder than one with the lower welding speed and rpm. It is important to note that all of the welds studied were essentially defect free and exhibited properties similar to each other when tested in transverse tension.

B. Flow Visualization by the Marker Insert Technique

The material flow in friction stir welds was visualized using the MIT. A total of six 2.7-mm-high, 1.8-mm-thick markers were placed in the weld path in order to gain both information about the overall material transport and detailed information about flow variations through the thickness of the plates. The marker inserts were made of AA5454-H32. Inserts were placed on both the advancing and the retreating sides, at three different heights, covering the top, middle, and bottom thirds of the plate. Inserts were staggered along the weld line so that the possibility of the mixing of markers from different positions was eliminated. The length of the markers was such that some of the markers, remote from the weld line, extended beyond the TMAZ and were not deformed by the welding process. Markers were placed by

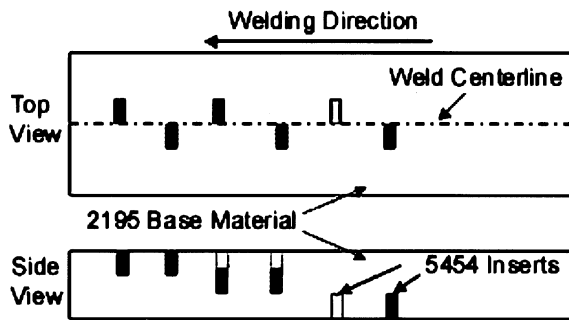


Fig. 3—Schematic drawings of the marker configuration. Three markers are placed on the advancing and retreating sides, respectively, at three different heights in the weld.

milling narrow slots into the faying surface and pressfitting the markers into the slots. For the markers that were placed in the middle third of the plate, an AA2195 shim of a size similar to that of the markers, was press fit into the upper third of the plate above the marker. Figure 3 shows schematically the configuration of the six inserts that, when put together, cover the total height and width of the welded zone.

The marker flow was elucidated by milling off successive slices, 0.25-mm thick, from the top surface of the weld. After each cut, the surface was etched with Keller's reagent,^[13] and digital images of the region surrounding each marker were obtained. Due to the etching process, the AA2195 base material (rich in copper) turns dark, whereas the AA5454 marker is relatively unaffected by the etchant. The pixel positions of the AA5454 markers were extracted from the digital images of each marker (a total of six) at each level (up to 32 per weld). Combining the data from all six markers, a three-dimensional flow visualization, similar to a computer tomography (CT) scan was obtained. The three-dimensional plot gives the final position of a thin layer, 1.8 mm thick, that was originally perpendicular to the welding direction.

IV. RESULTS

All welds had some general material flow patterns in common. The flow is not symmetric about the weld centerline. The flow patterns on the advancing and retreating sides are different. The bulk of the marker material was moved to a final position behind its original position and only a small amount of the material on the advancing side was moved to a final position in front of its original position. No material was transported further backward than 1 pin diameter behind its original position. The FSW can be roughly described as an in-situ extrusion process where the tool shoulder, the pin, the backing plate, and the cold base material form an extrusion die. Near the top of the weld, because of the shape of the tool, a substantial amount of material is moved from the retreating side of the weld to the advancing. This movement of material causes vertical mixing in the weld and a complex circulation of material around the longitudinal axis of the weld. The amount of the vertical material flow in the weld is strongly correlated with the temperature of the weld.

Figure 4 illustrates the process by which the images from separate markers are combined to provide a full three-dimensional view of material flow. Figure 4(a) is an image of the etched marker from the advancing side of weld 1 at a height

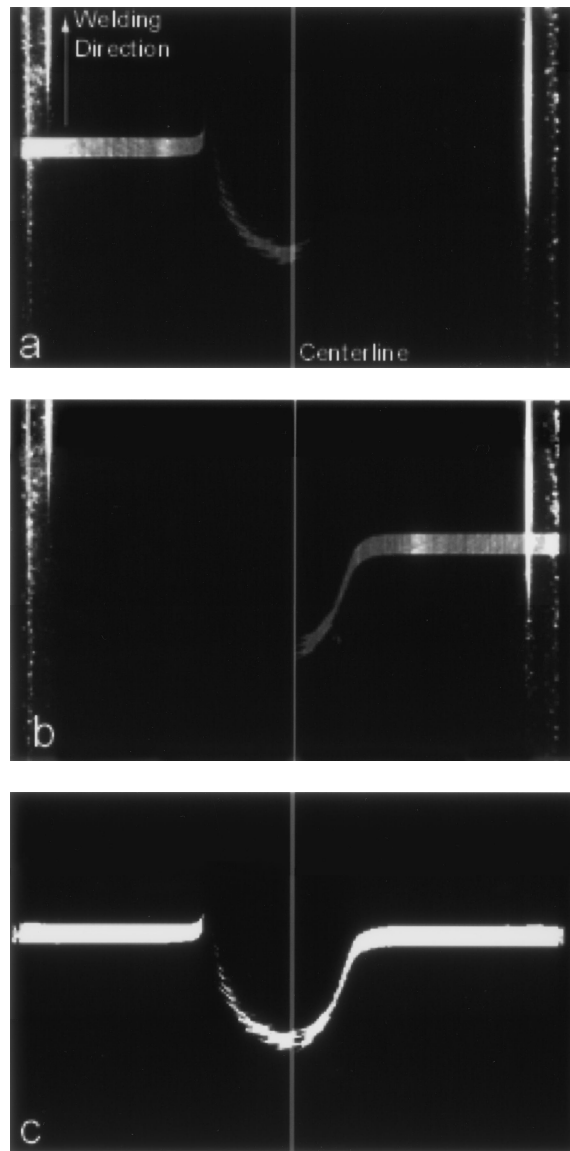


Fig. 4—(a) Picture of the advancing side marker at the middle height of weld 1. The bulk of the marker was transported against the welding direction. However, a small amount was moved forward at the edge of the pin. (b) Picture of the retreating side marker at the middle height of weld 1. This marker was transported against the welding direction, only. (c) The images of the (a) advancing and (b) retreating side markers are combined and binarized in (c) one image at the middle of weld 1 (0.61 mm/rev). The tool rotation was clockwise.

of 4 mm in the weld (near the mid-plane). Figure 4(b) is from the same height in weld 1, but is an image of the corresponding retreating side marker. The vertical line in both Figures 4(a) and (b) indicates the weld centerline. In Figure 4(c) the marker position data, extracted from Figures 4(a) and (b), have been combined into a single, binarized image. The images were combined so that the undeformed markers on the advancing and retreating sides were aligned (vertical alignment, as seen in the images) and so that the weld centerline from both images is coincident (horizontal alignment). No overlap between the advancing and retreating side markers was observed, but when combined, the two markers form a continuous path from the advancing to the retreating sides of the weld.

The procedure described in the preceding paragraph was

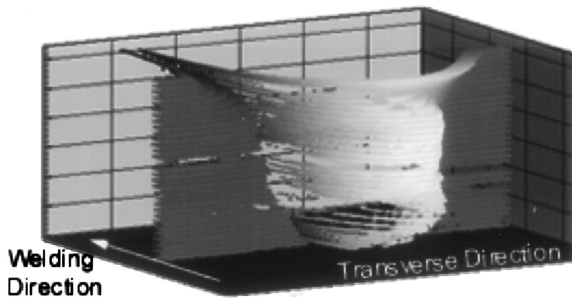


Fig. 5—Three-dimensional plot of the markers in weld 1 (0.61 mm/rev). The weld height (vertical axis) is magnified by a factor of 2.5. The markers are continuous after welding. The bulk of the material was transported against the welding direction behind its original position. Material transport in welding direction occurred only at the advancing side of the tool.

performed for each of 32 heights in each weld. The act of combining the data from all the detected marker positions at all 32 levels produces three-dimensional plots: one of these three-dimensional plots for weld 1 is shown in Figure 5. In Figure 5, the welding direction is into the plane of the paper, and the contour variable (represented by the shade of gray applied to a data point) is the y coordinate or position along the weld line. The z-axis of the plot is the height in the weld. One can see that the markers, assembled as described above, are continuous after welding. The bulk of the material is transported to a position behind its original one, but none of it by more than 1 pin diameter. In the top third of the weld, a substantial amount of material is transported forward of its original position (in the direction of welding), presumably by the action of the shoulder. This forward transport occurs for material originally on both the advancing and retreating sides; however, all of the material transported forward ends up on the advancing side of the weld. At lower levels in the weld, where the influence of the shoulder is diminished, only a small amount of marker material on the advancing side, slightly more than a pin radius from the weld centerline, was detected in front of its original position.

A three-dimensional plot, as shown in Figure 5, gives no information about the vertical mixing of the 32 layers. A projection of the marker positions onto a vertical plane in the welding direction is best suited for giving detailed information about the vertical material flow. Figure 6 shows the six markers before (Figure 6(a)) and after (Figure 6(b)) welding. A different gray scale level has been assigned to each marker so that the postwelding position of each marker may be determined in the plot. Note that the bulk of the material, *e.g.*, inside the pin diameter (dashed lines), was transported toward the observer, which is equivalent to the material transported backward relative to the welding direction. Material is pushed downward on the advancing side and moved upward toward the top at the retreating side within the pin diameter. It is believed that the counterclockwise material movement around the longitudinal axis is initiated by the material transport, due to the rotation of the tool's shoulder at the crown of the weld. At the crown, material from the retreating side was transported to the advancing side occupying space on the advancing side. Since FSW is a constant-volume process and the shoulder, the pin, and the undeformed base material restrict the flow path, the transport of material from the retreating to the advancing sides by the shoulder causes material from the top of the

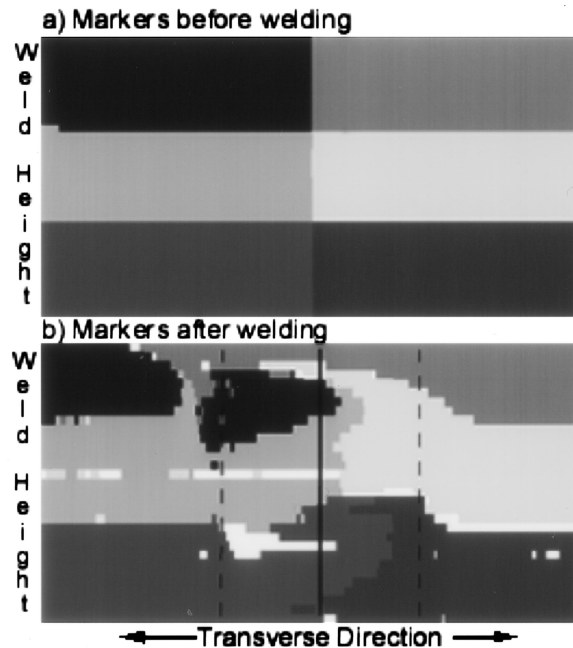


Fig. 6—Vertical mixing in weld 1 (0.61 mm/rev). The markers are projected in the vertical plane viewing in the welding direction. (a) The undeformed markers before welding and (b) the vertically mixed six markers after welding. The solid and the dashed lines denote the centerline and the pin diameter, respectively.

advancing side to move downward within the pin diameter. Closer to the root of the weld, the material transport is restricted by the backing plate; therefore, an upward motion is detected on the retreating side within and near the pin radius. The net result of the upward and downward material flows is a circulation about the longitudinal axis of the weld.

It is important to realize that the vertical circulation is a secondary motion, overlaid over the primary material transport around the rotating tool in the horizontal plane of the weld. The MIT does not directly provide information on the actual flow path of the material because it shows only the final position of the markers in the weld.

A. Weld Pitch Effects

In this section, the material flow in welds 1 through 4 is compared. The weld pitches for welds 2 through 4 indicate that each of these welds is hotter than weld 1 and that the hottest of these welds is weld 4, followed by weld 3, and then by weld 2. Since the projection of the markers onto the vertical plane in the welding direction offers the most valuable characterization of the welds, other views of the deformed markers are not shown in this section and in section, IV-B. Figure 7 shows the differences in the mixing for welds 2 through 4. The general pattern of material flow in each of welds 2 through 4 is consistent with the flow pattern described in the previous section for weld 1 (Figure 6). Material within the pin diameter experiences a counterclockwise rotation around the longitudinal axis during the transport backward to its final position in the weld. Outside the pin diameter, material is transported toward the top of the weld with flow into and opposite the welding direction on the advancing and retreating sides, respectively.

The effect of decreasing the weld pitch on the vertical

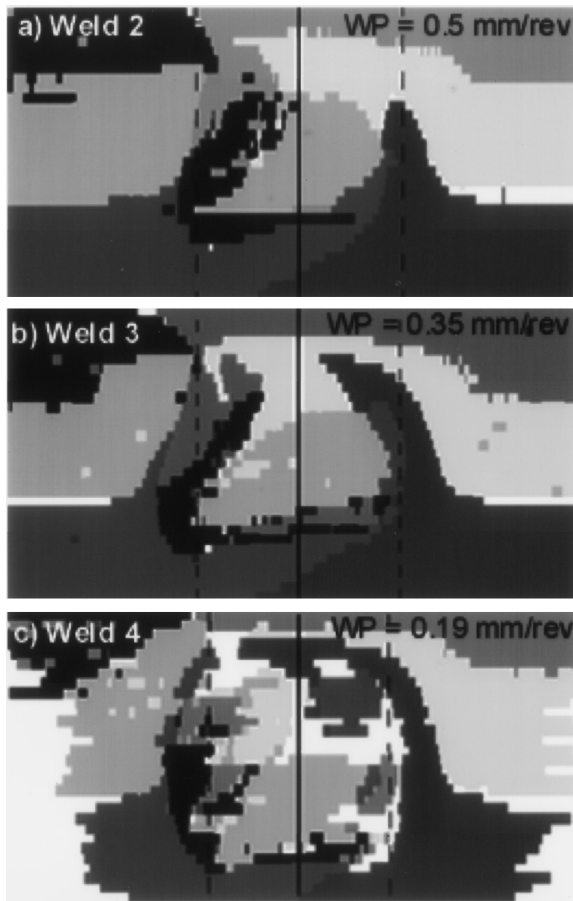


Fig. 7—Vertical mixing in (a) weld 2, (b) weld 3, and (c) weld 4. The mixing increases with decreasing weld pitch (increasing specific weld energy; here, increased tool rotation). The dashed lines denote the pin diameter, which was the same for the three welds.

mixing within the welds can be clearly observed by examining the final positions of the lower retreating side marker for welds 1 through 4 corresponding to weld pitch changes from 0.61 to 0.19 mm/rev (Figures 6 and 7). As the weld pitch decreases (and the weld energy increases) the portions of the bottom marker on the retreating side move higher and higher in the weld. In weld 1 (highest weld pitch), it can be seen that the retreating side bottom marker is being pushed upward; however, it does not reach the midplane (in z direction). In the weld with the lowest pitch, weld 4, the marker is entrained in the flow arm and is pulled completely across the top of the weld nugget. At the intermediate weld pitches, the markers are displaced upward, less than in weld 4 and more than in weld 1. In simple terms, the amount of vertical displacement of the retreating side bottom marker is inversely proportional to the weld pitch. Although the reason for the increased mixing that accompanies the decreasing weld pitch is not certain, the higher energy input may result in the softening of a greater volume of material in the weld zone and, as a result in the facilitation of the material transport. Alternatively, the increased vertical transport at the lower weld pitch may be due to the auguring effect of the threads acting on a given volume of material for a greater time (rotation is such that the threads push the material down). Although not shown here, a well-defined interface between material originally on opposite sides of

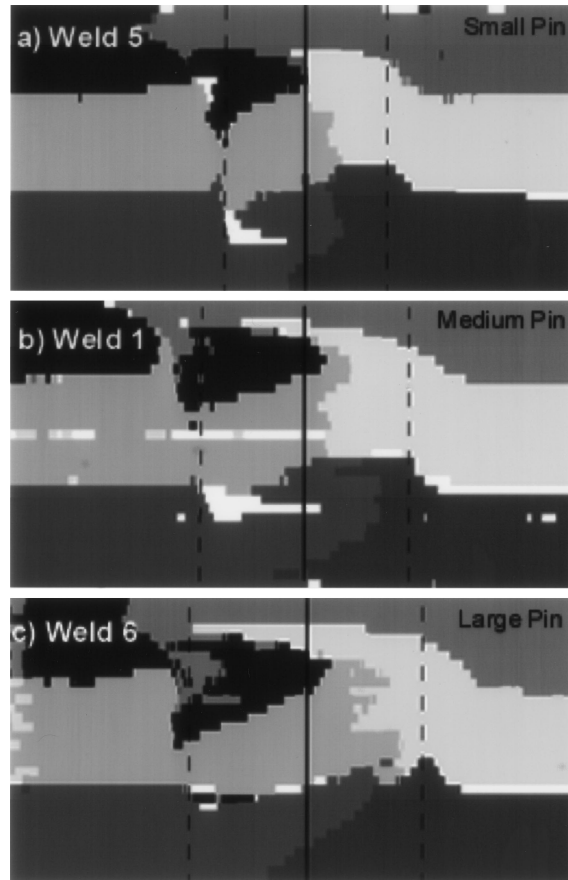


Fig. 8—Vertical mixing for different pin diameters in (a) weld 5, (b) weld 1, and (c) weld 6. Increasing the pin diameter increases the vertical mixing. Almost no vertical mixing occurred in (a) weld 5, *i.e.*, the interfaces between the three layers are almost horizontal. In (b) weld 1 and (c) weld 6, an increasing amount of material was pushed downward on the advancing side and upward on the retreating side.

the weld centerline is present in the cold welds (welds 1, 5, and 6), but cannot be seen in the welds that were performed at a lower weld pitch.

B. Pin Diameter Effects

Welds 1, 5, and 6 were performed with the same tool rotation rates and welding speeds (weld pitch = 0.61 mm/rev), but with different tools, all having the same shoulder diameter of 25.4 mm. As shown in Table I, Welds 1, 5, and 6 were made using pin diameters of 9.9, 7.8, and 12 mm, respectively. In Figures 8(a) through (c), the final marker positions are projected onto the y - z plane of the weld, so that the transport of the marker material may be observed. In Figure 8(a), weld 5, the interface between the advancing and retreating side markers is near the weld centerline in the lower two-thirds of the weld. Only near the crown of the weld, where the influence of the shoulder is important, does a substantial amount of material cross the centerline. In (Figure 8(b), weld 1, made using the 9.9-mm-diameter pin, a larger amount of material crosses the centerline in the bottom third of the weld due to the circulation about the longitudinal axis of the weld. Figure 8(c) shows that in weld 6, a substantial amount of material crosses the weld centerline from advancing to retreating sides in the bottom

two-thirds of the weld. The increased material transport across the weld centerline that results from the use of larger diameter pins may result from an increase in weld energy at constant rotational and welding speeds. It seems likely that more work goes into a weld made with a large pin than with a small pin: the nugget size increases with the pin size, which indicates that more material undergoes severe plastic deformation when a large pin is used. Torque measurements have not yet been made during these particular welds; however, the measurement of the required torque would shed light on this phenomenon.

V. SUMMARY AND CONCLUSIONS

Friction-stir butt welds were analyzed with respect to the material flow for different welding parameters. The material transport was visualized using marker inserts in the faying surface of the two plates to be welded. The MIT technique gives insight into the TMAZ by means of reconstruction of the piecewise cutoff welded zone. As a result, full three-dimensional plots of the deformed markers provide a good, qualitative characterization of the material flow in these FSWs. However, this technique does not reconstruct the actual flow path of the material.

The tool rotation produces deformation heating in the workpiece leading to a reduction in the flow stress of the base material, allowing the material in the weld zone to flow. Increasing the heat input by the tool results in reduced flow stresses and increases, as a side effect, the mobility of material in the weld. The material transport in FSW is a result of the two tool motions, translation and rotation. The bulk of the material is moved around the pin to final positions behind its original positions. The “stirring” of material occurs only at the top of the weld where the material transport

is directly influenced by the rotating tool shoulder that moves material from the retreating side clockwise around the pin to the advancing side. The extrusion around the pin combined with the stirring action at the top of the weld produces within the pin diameter a secondary, vertical, counterclockwise, circular motion around the longitudinal axis of the weld. Outside the pin diameter, material is pushed toward the crown of the weld. The maximum material transport against the welding direction was not larger than 1 pin diameter.

REFERENCES

1. W.M. Thomas, E.D. Nicholas, J.C. Needham, M.G. Church, P. Templesmith, and C.J. Dawes: International Patent Application No. PCT/GB92/02203 and GB Patent Application No. 9125978.9, 1991.
2. M.W. Mahoney, C.G. Rhodes, and W.H. Bingel: *Metall. Mater. Trans. A*, 1998, vol. 29A, pp.1955-64.
3. T.J. Lienert and R.J. Grylls: *Proc. 1st Int. Symp. FSW*, Thousand Oaks, CA, 1999.
4. A.V. Strombeck, J.F. dos Santos, F. Torster, P. Laureano, and M. Koçak: *Proc. 1st Int. Symp. FSW*, Thousand Oaks, CA, 1999.
5. C. Dalle Donne, R. Braun, G. Staniek, A. Jung, and W.A. Kaysser: *Mater.-Wiss. u. Werkstofftech.*, 1998, vol. 29, pp. 609-17.
6. O.T. Midling: *Proc. 4th Int. Conf. Aluminum Alloys*, Atlanta, GA, 1994, T.H. Sanders, Jr. and E.A. Starke, Jr., eds., Georgia Institute of Technology, School of Materials Science and Engineering, Atlanta, GA.
7. Y. Li, L.E. Murr, and J.C. McClure: *Scripta Mater.*, 1999, vol. 40, pp. 1041-46.
8. K. Colligan: *Welding J.*, 1999, vol. 65, pp. 229-37.
9. A.P. Reynolds, T.U. Seidel, and M. Simonsen: *Proc. 1st Int. Symp. FSW*, Thousand Oaks, CA, 1999.
10. A.P. Reynolds: *Sci. Technol. Welding Joining*, 2000, vol. 5, pp. 120-24.
11. T.U. Seidel and A.P. Reynolds: *Proc. SECTAM-XX*, Pine Mountain, GA, 2000.
12. A.P. Reynolds and W. Tang: University of South Carolina, Columbia, SC, unpublished research, 2001.
13. *Metals Handbook*, 8th ed., vol. 8, *Metallography, Structures and Phase Diagrams*, ASM, Metals Park, OH, 1973, p. 124.